AMERICAN SOCIETY FOR MICROBIOLOGY | Microbiology Spectrum

RESEARCH ARTICLE

Coordinated and Distinct Roles of Peptidoglycan Carboxypeptidases DacC and DacA in Cell Growth and Shape Maintenance under Stress Conditions

Umji Choi,[a] Si Hyoung Park,[a] Han Byeol Lee,[a] Ji Eun Son,[a] Chang-Ro Lee[a,b]

[a]Department of Biological Sciences, Myongji University, Yongin, Gyeonggido, Republic of Korea
[b]The Natural Science Research Institute, Myongji University, Yongin, Gyeonggido, Republic of Korea

ABSTRACT Peptidoglycan (PG) is an essential bacterial architecture pivotal for shape maintenance and adaptation to osmotic stress. Although PG synthesis and modification are tightly regulated under harsh environmental stresses, few related mechanisms have been investigated. In this study, we aimed to investigate the coordinated and distinct roles of the PG DD-carboxypeptidases (DD-CPases) DacC and DacA in cell growth under alkaline and salt stresses and shape maintenance in *Escherichia coli*. We found that DacC is an alkaline DD-CPase, the enzyme activity and protein stability of which are significantly enhanced under alkaline stress. Both DacC and DacA were required for bacterial growth under alkaline stress, whereas only DacA was required for growth under salt stress. Under normal growth conditions, only DacA was necessary for cell shape maintenance, while under alkaline stress conditions, both DacA and DacC were necessary for cell shape maintenance, but their roles were distinct. Notably, all of these roles of DacC and DacA were independent of LD-transpeptidases, which are necessary for the formation of PG 3-3 cross-links and covalent bonds between PG and the outer membrane lipoprotein Lpp. Instead, DacC and DacA interacted with penicillin-binding proteins (PBPs)—DD-transpeptidases—mostly in a C-terminal domain-dependent manner, and these interactions were necessary for most of their roles. Collectively, our results demonstrate the coordinated and distinct novel roles of DD-CPases in bacterial growth and shape maintenance under stress conditions and provide novel insights into the cellular functions of DD-CPases associated with PBPs.

IMPORTANCE Most bacteria have a peptidoglycan architecture for cell shape maintenance and protection against osmotic challenges. Peptidoglycan DD-carboxypeptidases control the amount of pentapeptide substrates, which are used in the formation of 4-3 cross-links by the peptidoglycan synthetic DD-transpeptidases, penicillin-binding proteins (PBPs). Seven DD-carboxypeptidases exist in *Escherichia coli*, but the physiological significance of their redundancy and their roles in peptidoglycan synthesis are poorly understood. Here, we showed that DacC is an alkaline DD-carboxypeptidase for which both protein stability and enzyme activity are significantly enhanced at high pH. Strikingly, DD-carboxypeptidases DacC and DacA physically interacted with PBPs, and these interactions were necessary for cell shape maintenance as well as growth under alkaline and salt stresses. Thus, cooperation between DD-carboxypeptidases and PBPs may allow *E. coli* to overcome various stresses and to maintain cell shape.

KEYWORDS peptidoglycan, peptidoglycan hydrolase, DD-carboxypeptidase, cell shape, stress adaptation, cell morphology, penicillin-binding proteins, LD-transpeptidase, alkaline stress, DacC

Peptidoglycan (PG) is an essential bacterium-specific architecture found in most Gram-negative and Gram-positive bacteria. PG not only determines bacterial shape but also plays an important role in providing protection against turgor pressure (1, 2).

Editor Cristina Solano, Navarrabiomed-Universidad Pública de Navarra (UPNA)-Complejo Hospitalario de Navarra (CHN), IdiSNA

Address correspondence to Chang-Ro Lee, crlee@mju.ac.kr.

The authors declare no conflict of interest.

Received 8 January 2023
Accepted 9 April 2023
Published 26 April 2023

PG is a mesh-like polymer composed of long linear polysaccharide chains formed by alternating connections between two amino sugar derivatives, *N*-acetylglucosamine and *N*-acetylmuramic acid (1). The cross-links between polysaccharide chains are formed by covalent bonds between the peptide chains, which are attached to *N*-acetylmuramic acid (1). The linear polysaccharide chain is formed by periplasmic enzymes with glycosyltransferase activity, such as the shape, elongation, division, and sporulation (SEDS) family of proteins and class A penicillin-binding proteins (PBPs) (2, 3). The cross-links between polysaccharide chains are facilitated by periplasmic enzymes with DD-transpeptidase activity, such as class A or B PBP (aPBP or bPBP, respectively), which results in the formation of 4-3 cross-links (2). The cross-links between polysaccharide chains can also be formed by LD-transpeptidases, which results in the formation of 3-3 cross-links (4). In most bacteria, the vast majority (>90%) of PG cross-links are the 4-3 cross-links, but in a few bacteria, such as *Mycobacterium tuberculosis*, the portion of 3-3 cross-links is considerably high, accounting for >60% of the PG cross-links (5).

Cross-linked PG in the periplasm is degraded by diverse PG hydrolases, namely, amidases, lytic transglycosylases, endopeptidases, and carboxypeptidases (6–8). PG amidases that hydrolyze the lactylamide bond between *N*-acetylmuramic acid and the peptide chain are associated with cytokinetic ring contraction at the division site (9, 10). Lytic transglycosylases that cleave the β-1,4-glycosidic bond between *N*-acetylglucosamine and *N*-acetylmuramic acid are known to play important roles in PG quality control (11), termination of PG glycan polymerization (12–14), and establishment of flagellar and type VI secretion architectures (15, 16). PG endopeptidases that cleave within the cross-bridged peptide chains are known to function as space makers that cleave the cross-linked peptide chains for the insertion of newly synthesized PG strands (17–20). All PG hydrolases showed strong redundancy. For example, *Escherichia coli* has eight enzymes that exhibit lytic transglycosylase activity in the periplasm (13, 14) and eight enzymes with PG endopeptidase activity (18, 20). Although the physiological significance of PG hydrolase redundancy has not yet been fully elucidated, it is thought to enable the maintenance of PG synthesis and degradation under harsh extracellular stresses (10, 18, 21, 22). Like MepK, which exclusively cleaves the 3-3 cross-links, an enzyme with the cleavage specificity has also been reported (20).

PG DD-carboxypeptidases (DD-CPases) remove the C-terminal fifth D-alanine (D-Ala) of the peptide chains (L-Ala–D-Glu–*meso*-Dap–D-Ala–D-Ala) (7). After the removal of the terminal D-Ala residue, the remaining four amino acids of the peptide chain can be cross-linked (3-3 cross-links) with the adjacent peptide chain by LD-transpeptidases (LdtD and LdtE), covalently attached to an abundant outer membrane (OM) lipoprotein Lpp (Braun's lipoprotein) by other LD-transpeptidases (LdtA, LdtB, and LdtC), or cross-linked (4-3 cross-links) with the adjacent peptide chain by DD-transpeptidases (4, 7). Although the roles of DD-CPases associated with LD-transpeptidases have been extensively studied, their roles in cell shape maintenance and PG synthesis regulation are poorly understood (3). Seven proteins have DD-CPase activity in *E. coli* (6, 7). DacA (also called PBP5) is the most abundant DD-CPase and is expressed primarily during early exponential growth in *E. coli* (23, 24). The loss of DacA results in aberrant cell morphologies, and additional deletions of at least two other DD-CPases worsen these morphological defects (25, 26). DacD (also called PBP6b) was identified as an acidic DD-CPase, whose expression and activity increased at acidic pH (21). DacC (also called PBP6a) was recently shown to be involved in overcoming severe OM assembly defects by increasing the number of 3-3 cross-links of PG (27). DacD and DacC are expressed in the mid-exponential growth and stationary phases, respectively (23, 28). DacA, DacC, and DacD are membrane-anchored proteins via their C-terminal amphiphilic α-helix domains (29), and this domain is important for the morphological functioning of PBP5 (30), its localization at the cell division site (30, 31), and β-lactam resistance (32, 33).

In this study, we investigated the coordinated and distinct functions of the DD-CPases DacC and DacA in growth under alkaline and salt stresses as well as cell shape maintenance. We found that DacC is an alkaline DD-CPase the protein stability and

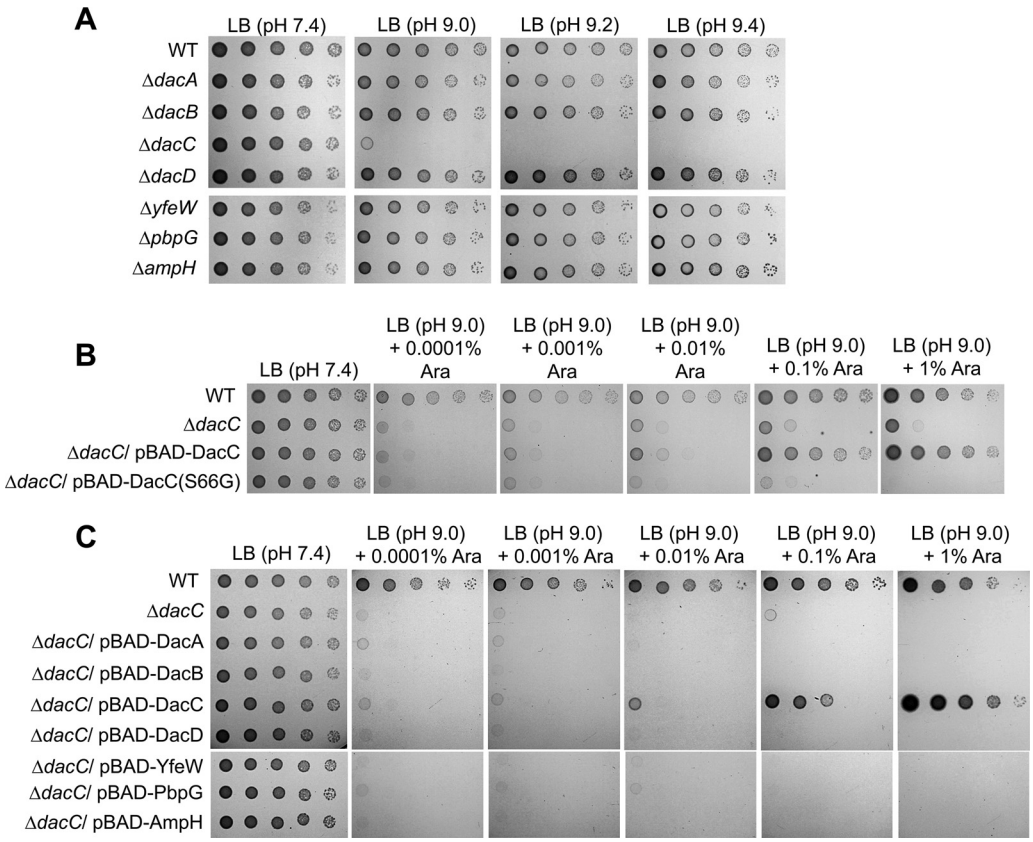

FIG 1 The activity of DacC is required for growth under alkaline stress conditions. (A) Sensitivity of the *dacC* mutant to alkaline pH. The wild-type (WT) and indicated mutant cells were serially diluted from 10^8 to 10^4 cells/mL in 10-fold steps and spotted onto an LB plate or LB plates at the indicated pH. (B) Complementation of alkaline sensitivity of the *dacC* mutant. The cells of the indicated strains were serially diluted from 10^8 to 10^4 cells/mL in 10-fold steps and spotted onto an LB plate and LB plates at pH 9.0 containing the indicated concentrations of arabinose. (C) Complementation of alkaline sensitivity of the *dacC* mutant by other DD-CPases. The cells of the indicated strains were serially diluted from 10^8 to 10^4 cells/mL in 10-fold steps and spotted onto an LB plate and LB plates at pH 9.0 containing the indicated concentrations of arabinose.

enzyme activity of which are significantly increased at high pH. Both DacC and DacA were necessary for overcoming high pH stress, whereas only DacA was necessary for bacterial growth under salt stress. Both DacC and DacA play important roles in maintaining cell shape, but their roles are distinct. Notably, all of these functions of DacC and DacA were not associated with LD-transpeptidases, but with DD-transpeptidases (PBPs). We showed the C-terminal domain-dependent interactions between DD-CPases and PBPs. Therefore, our study suggests a model whereby DD-CPases and PBPs cooperate for growth under stress conditions and cell shape maintenance.

RESULTS

DacC activity is required for growth at alkaline pH. To analyze the role of DD-CPases in overcoming alkaline stress, we examined the alkaline sensitivity of the DD-CPase-deleted mutant strains. The *dacC* mutant had a 4-log plating defect on an LB plate at pH 9.0 and does not grow at pH 9.2 or 9.4, whereas the growth of other mutant cells was comparable to that of the wild-type (WT) cells under high-pH conditions (Fig. 1A; see Fig. S1A in the supplemental material). This phenotype was complemented by ectopic expression of DacC under the pBAD plasmid with an arabinose-inducible promoter (Fig. 1B; Fig. S1B) but not by the expression of a DacC(S66G) mutant protein, in which the serine residue of the active site is substituted for with glycine (21). These results indicate that DD-CPase activity of DacC is necessary for cell growth under alkaline stress. We examined whether the overexpression of other DD-CPases

could complement the phenotype of the *dacC* mutant. In the presence of 1% arabinose, DacC fully complemented the phenotype of the *dacC* mutant, whereas other proteins did not complement it at all (Fig. 1C; Fig. S1C), suggesting that DacC has a distinct role in overcoming alkaline stress.

Increased enzyme activity and protein stability of DacC under alkaline stress. A systematic analysis of the protein levels in *E. coli* showed that the protein level of DacC was significantly lower than that of other DD-CPases under normal growth conditions (24). However, in this study, only the growth of the *dacC* mutant was inhibited under alkaline stress and this phenotype was complemented only by the expression of DacC (Fig. 1). To understand the distinct role of DacC under alkaline stress, we examined enzyme activity and expression levels of DacC under alkaline stress. A previous study also prompted us to investigate this point, showing that the DD-CPase activity of DacD was higher at low pH than at neutral pH, and its protein level increased at low pH (21). An *in vitro* experiment using a bacterial cell wall analog showed that the enzymatic activity of DacC was more than doubled at high pH than at neutral pH (Fig. 2A). We examined the mRNA level of the *dacC* gene at high pH. The transcript level of *dacC* did not change significantly under alkaline stress compared to that under normal conditions (Fig. 2B). The protein level of DacC was also examined under high-pH conditions. The protein level of DacC increased by more than 3-fold under alkaline stress conditions than under normal conditions (Fig. 2C and D). Additionally, we checked the protein levels of DacC paralogs, DacA and DacD. The protein level of DacA did not change under alkaline stress conditions, whereas DacD was strongly diminished under alkaline stress conditions (Fig. 2C and D). Therefore, these results indicate that DacC is a DD-CPase that is specialized for growth at alkaline pH. To understand why the protein level of DacC increased under alkaline stress conditions, we estimated the protein stability of DacC (Fig. 2E). The half-life of DacC was prolonged by more than twice the normal length under alkaline stress (~66 min) than under normal conditions (~29 min) (Fig. 2F), indicating that the increased protein level of DacC under alkaline stress is mediated by the decreased degradation rate of DacC.

DacA plays an auxiliary role in growth under alkaline stress and a pivotal role in growth under salt stress. Because the protein level of DacA was consistently maintained under alkaline stress (Fig. 2C), its role in growth under alkaline stress was examined. Although the *dacA* single mutant showed normal growth under alkaline stress (Fig. 1A), additional deletion of DacA in the *dacC* mutant worsened the growth defect of the *dacC* mutant under alkaline stress (Fig. 3A; and Fig. S2A). The additional deletion of DacD in the *dacC dacA* double mutant did not affect bacterial growth under alkaline stress. This phenotype, caused by the additional deletion of DacA in the *dacC* mutant, was fully complemented by the ectopic expression of DacA (Fig. 3B; Fig. S2B). These results indicate that DacA plays an accessory role in overcoming alkaline stress. The *dacA* mutant also did not grow well on high-salt medium, which was fully complemented by the ectopic expression of DacA (Fig. 3C; Fig. S2C). This phenotype was not detected in the other six DD-CPase mutants, including the *dacC* mutant (32), and additional deletions of DacC and DacD did not increase salt sensitivity of the *dacA* mutant (Fig. S2D), indicating that only DacA was associated with this phenotype. These data suggest that DacA is required for overcoming alkaline and salt stresses.

Inactivation of DacA and DacC leads to distinct shape abnormalities. DacA has been known to be important for morphological maintenance (25, 30, 34). Cells with an abnormal morphology, such as branched or filamentous shapes, were detected in the *dacA* mutant in lysogeny broth (LB) medium (Fig. 3D). These morphological defects were fully complemented by the ectopic expression of DacA. The *dacC* mutant did not exhibit any morphological defects under normal growth conditions (Fig. 4A). Next, we examined the effect of alkaline stress on the morphology of the *dacC* and *dacA* mutants. Notably, under alkaline stress, the *dacC* mutant exhibited a spherical shape, whereas the *dacA* mutant exhibited a filamentous shape (Fig. 4A). These morphological phenotypes were complemented by the ectopic expression of each protein (Fig. 4B and C). It is noteworthy that cells with abnormal morphology were observed in the

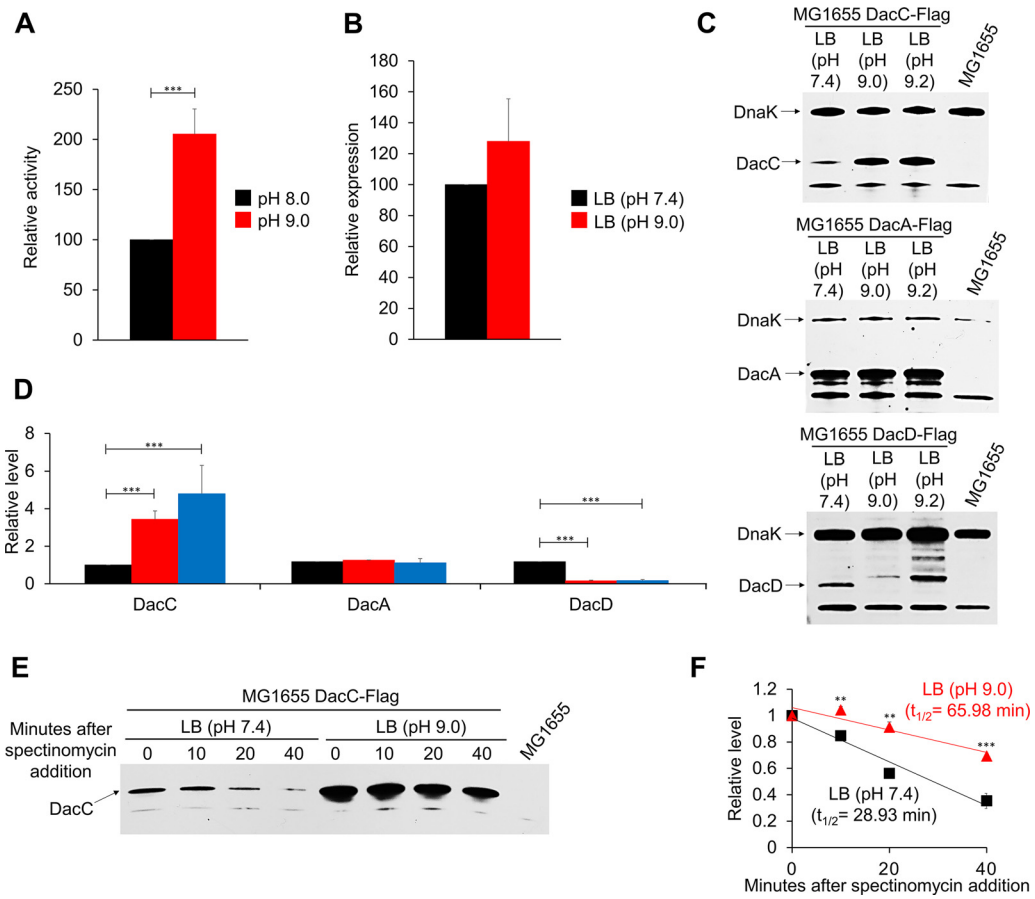

FIG 2 The enzyme activity and protein stability of DacC are enhanced under alkaline stress conditions. (A) Increased enzymatic activity of DacC at an alkaline pH. The enzymatic activity of purified DacC was measured using the bacterial cell wall analog diacetyl-L-Lys-D–Ala–D-Ala (AcLAA). Purified protein (1 μM) was incubated at 37°C for 60 min with 50 mM Tris-HCl (pH 8.0 or 9.0) containing 1 mM AcLAA. The amount of D-Ala released by DacC was measured using horseradish peroxidase and Amplex Red. Data were obtained from three independent experiments. ***, $P < 0.001$. (B) Relative transcript levels of the *dacC* gene in LB medium (black bar) and LB medium at pH 9.0 (red bar). Total mRNA was extracted from MG1655 cells grown in the indicated media to the early exponential phase (OD_{600} = 0.4). Data were obtained from three independent experiments. mRNA levels were normalized to the concentration of 16S rRNA. (C) Protein levels of DacC, DacA, and DacD in LB medium or LB media at the indicated pH. Western blot analysis with anti-Flag and anti-DnaK antibodies was performed using MG1655 DacC-Flag, DacA-Flag, or DacD-Flag cells grown in the indicated media to the early exponential phase (OD_{600} = 0.4). DnaK was used as the loading control. The exact position of DacD was determined by Western blotting with the anti-Flag antibody. The mixture of anti-Flag and anti-DnaK antibodies cross-reacted with other nonspecific bands that were not characterized. (D) Quantification of the protein levels in panel C plotted as relative levels: black bars, LB; red bars, LB at pH 9.0; blue bars, LB at pH 9.2. Error bars represent the standard deviation from triplicate measurements. ***, $P < 0.001$. (E) *In vivo* degradation assay of DacC. MG1655 DacC-Flag cells were grown in LB medium or LB medium at pH 9.0 to the early exponential phase (OD_{600} = 0.4). Spectinomycin was added to each culture to a final concentration of 200 μg/mL to block protein synthesis, and 6×10^7 cells were harvested at the indicated time points for Western blotting. Each experiment was performed in triplicate, and a representative image is shown. (F) The normalized signal at the time of spectinomycin addition was set as 1, and the change in signal intensity at each time point was plotted for each medium: black, LB; red, LB (pH 9.0). Error bars represent the standard deviation from the triplicate measurements. **, $P < 0.01$; ***, $P < 0.001$.

dacA mutant at neutral pH but not at the alkaline pH range of 8.6 to 8.8 (Fig. 4A). Under salt stress, the *dacA* mutant exhibited severely branched irregular shapes (Fig. S2E). These results indicate that both DacA and DacC are necessary for shape maintenance, but their roles in morphology are distinct.

The roles of DacC and DacA in cell growth under stress conditions and morphology maintenance are not associated with LD-transpeptidases. After the removal of the fifth D-Ala by DD-CPases, PG stem peptides can be covalently attached to Lpp lipoproteins or adjacent PG peptides by LD-transpeptidases (4). The attachment of Lpp lipoproteins is catalyzed by LdtABC (4), whereas the formation of 3-3 cross-links is catalyzed by LdtDE (35, 36). Thus, we examined the relationship between LD-transpeptidases and

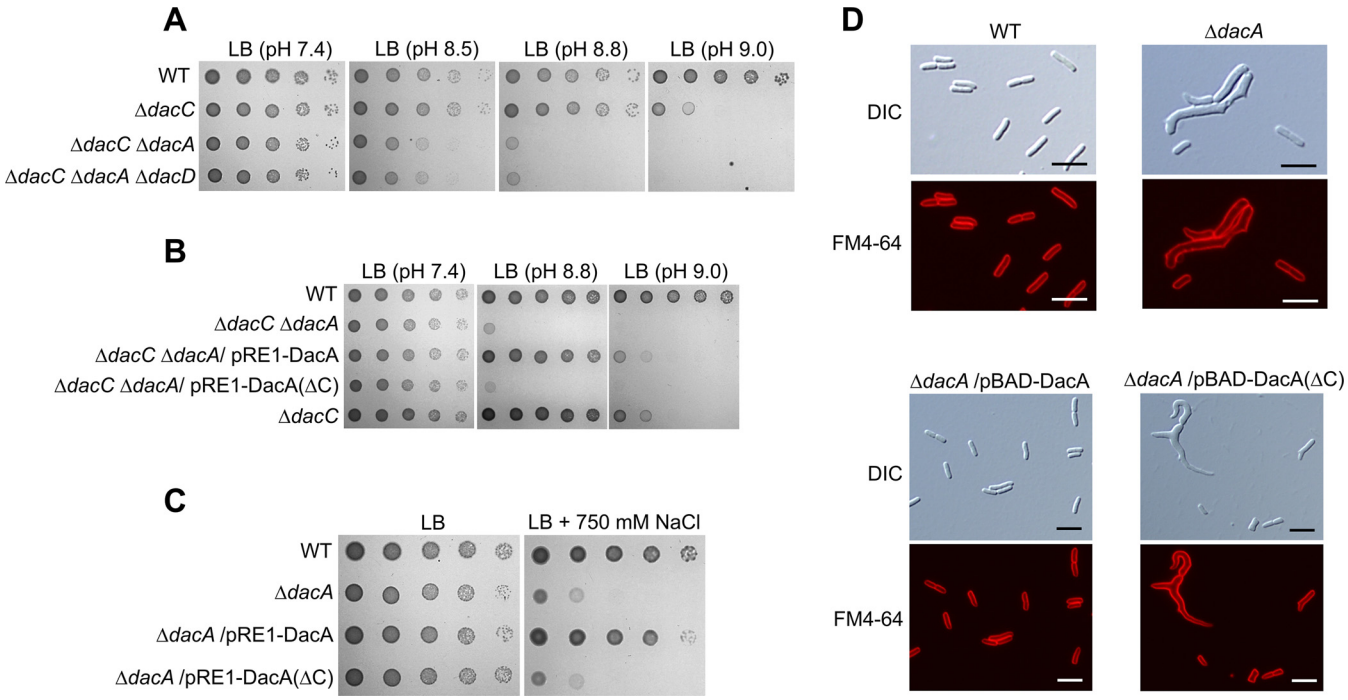

FIG 3 Effects of DacA depletion on morphological maintenance and cell growth under alkaline and salt stresses. (A) Increased sensitivity of the *dacC* mutant to alkaline pH by additional deletion of the *dacA* gene. The wild-type (WT) and indicated mutant cells were serially diluted from 10^8 to 10^4 cells/mL in 10-fold steps and spotted onto an LB plate or LB plates at the indicated pH. (B) Complementation of alkaline sensitivity of the *dacC dacA* double mutant. The cells of the indicated strains were serially diluted from 10^8 to 10^4 cells/mL in 10-fold steps and spotted onto an LB plate and LB plates at the indicated pH. (C) Salt sensitivity of the *dacA* mutant. The wild-type and indicated mutant cells were serially diluted from 10^8 to 10^4 cells/mL in 10-fold steps and spotted onto an LB plate (171 mM NaCl) or an LB plate containing 750 mM NaCl. (D) Morphological defects of the *dacA* mutant in LB medium. The indicated cells grown in LB medium containing 0.2% arabinose were stained with FM4-64 (red) and then spotted onto a 1% agarose pad. Scale bars, 5 μm.

roles of DacA and DacC identified in this study. Cells defective in all LD-transpeptidases showed normal growth under alkaline stress, comparable to that of the WT strain (Fig. 5A; Fig. S3A). Additionally, the deletion of DacC in the Δ*ldtABCDE* strain caused sensitivity to alkaline stress up to the same level as that of the *dacC* mutant (Fig. 5A; Fig. S3A), indicating that the alkaline sensitivity of the *dacC* mutant is not associated with LD-transpeptidases. Likewise, the salt sensitivity of the *dacA* mutant was not associated with LD-transpeptidases (Fig. 5B; Fig. S3B).

The *dacA* mutant showed an abnormal shape in LB medium at pH 7.4 and a filamentous shape in alkaline LB medium (Fig. 3D and 4A), whereas the *dacC* mutant showed a spherical shape in alkaline LB medium (Fig. 4A). However, these morphological abnormalities were not observed in the Δ*ldtABCDE* strain, and the additional deletion of DacA and DacC in the Δ*ldtABCDE* strain phenocopied the morphological defects of the *dacA* and *dacC* mutants, respectively (Fig. 5C). Collectively, these results demonstrate that the physiological roles of DacA and DacC in growth under stress conditions and morphology are not mediated by LD-transpeptidase-related functions.

C-terminal membrane-anchoring domains of DacC and DacA are indispensable for their most cellular functions, but not their enzymatic activities. DacC has a membrane-anchoring domain at its C terminus, and a lack of this domain produces a soluble protein (37, 38). We constructed a DacC(ΔC) mutant protein defective in the membrane-anchoring domain to investigate the role of this domain in cell growth under alkaline stress. Although the DD-CPase activity of DacC(ΔC) was significantly higher than that of WT DacC, regardless of pH (Fig. 6A), DacC(ΔC) hardly complemented the alkaline sensitivity of the *dacC* mutant (Fig. 6B; Fig. S4A). DacC(ΔC) did not complement morphological changes in the *dacC* mutant under alkaline stress (Fig. 4B; Fig. S4B). To confirm the requirement of the C-terminal domain of DacC in its cellular functions, we constructed a strain defective for the C-terminal domain of chromosomal DacC, MG1655 DacC(ΔC)-Flag. Although the expression level of DacC(ΔC) was higher

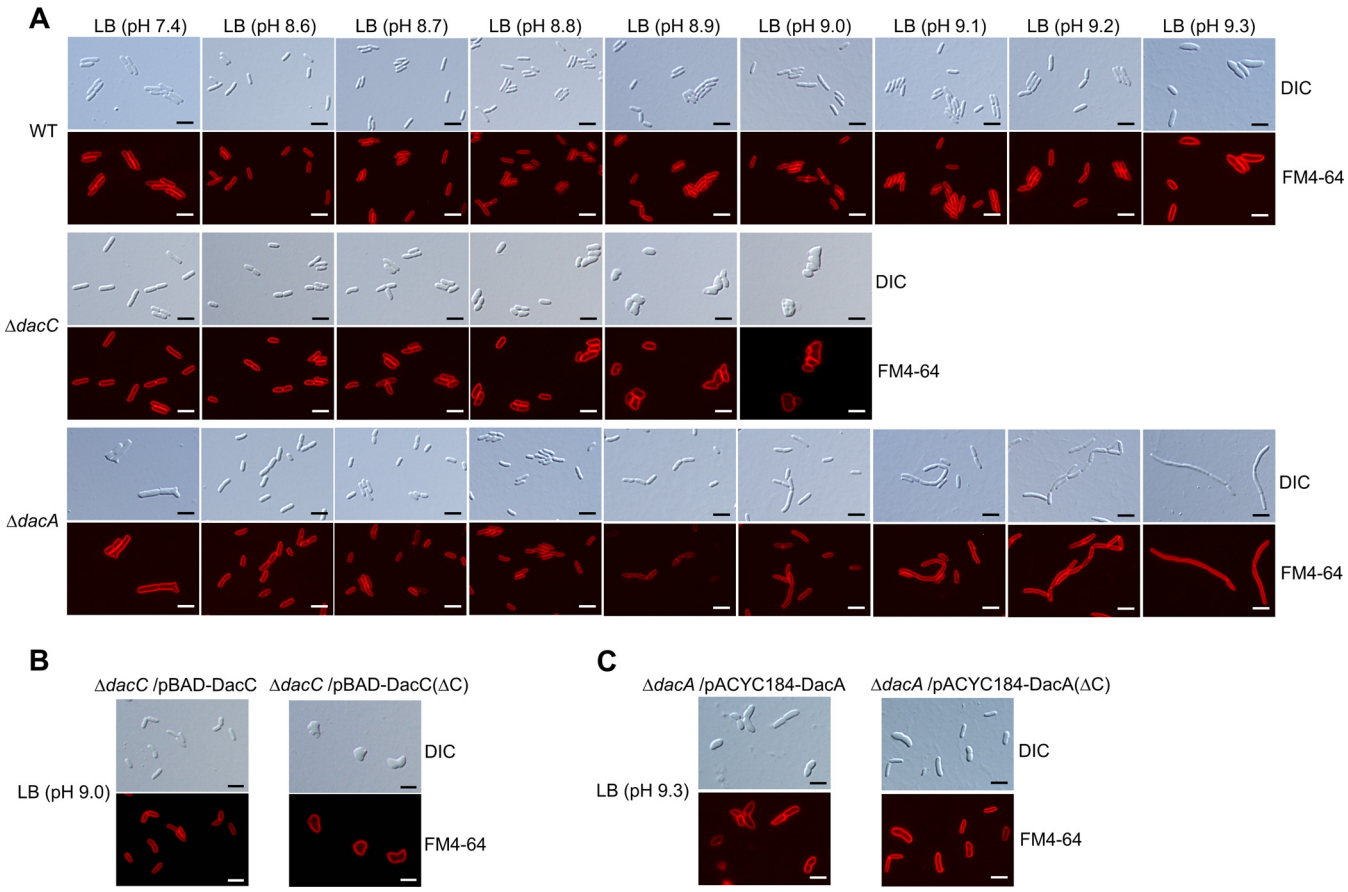

FIG 4 Distinct morphological changes of *dacC* and *dacA* mutants under alkaline stress conditions. (A) Cell shapes of *dacC* and *dacA* mutants under alkaline stress conditions. The indicated cells grown in LB medium or LB media at the indicated pH were stained with FM4-64 (red) and then spotted onto a 1% agarose pad. Scale bars, 5 μm. (B) Complementation of spherical shape of the *dacC* mutant under alkaline stress conditions. The indicated cells grown in LB medium at pH 9.0 containing 0.2% arabinose were stained with FM4-64 (red) and then spotted onto a 1% agarose pad. Scale bars, 5 μm. (C) Complementation of filamentous shape of the *dacA* mutant under alkaline stress conditions. The indicated cells grown in LB medium at pH 9.3 were stained with FM4-64 (red) and then spotted onto a 1% agarose pad. Scale bars, 5 μm.

than that of DacC (Fig. 7A), MG1655 DacC(ΔC)-Flag cells were highly sensitive to alkaline stress (Fig. 7B; Fig. S5A) and exhibited morphological changes under alkaline stress (Fig. 7C), similar to the *dacC* mutant. These results imply that retaining only the DD-CPase activity of DacC is not sufficient for its intracellular role and that another factor is required for its function.

The role of the C-terminal membrane-anchoring domain of DacA was also analyzed. A previous report showed that DD-CPase activity of DacA(ΔC) was significantly higher than that of WT DacA (32). DacA(ΔC) did not complement the alkaline and salt sensitivities of the *dacA* mutant or morphological defects in LB medium (Fig. 3). However, DacA(ΔC) fully complemented the filamentous morphology of the *dacA* mutant under alkaline stress (Fig. 4C). Additionally, these results were confirmed by using a strain defective for the C-terminal domain of chromosomal DacA, MG1655 DacA(ΔC)-Flag. Although the expression level of DacA(ΔC) was comparable to that of DacA (32), MG1655 DacA(ΔC)-Flag cells were highly sensitive to alkaline and salt stresses (Fig. 7D and E; Fig. S5B and C) and exhibited morphological defects in LB medium (Fig. 7C). However, MG1655 DacA(ΔC)-Flag cells did not exhibit filamentous morphology under alkaline stress (Fig. 7C). Taken together, these results demonstrate that the DD-CPase activities of DacC and DacA are not solely sufficient for most intracellular roles and that other factors are required for their functions.

DacC and DacA directly interact with PBPs, mostly in a C-terminal domain-dependent manner. In a previous study, we demonstrated that DacA directly interacts with PBPs in a C-terminal domain-dependent manner (32). To determine whether

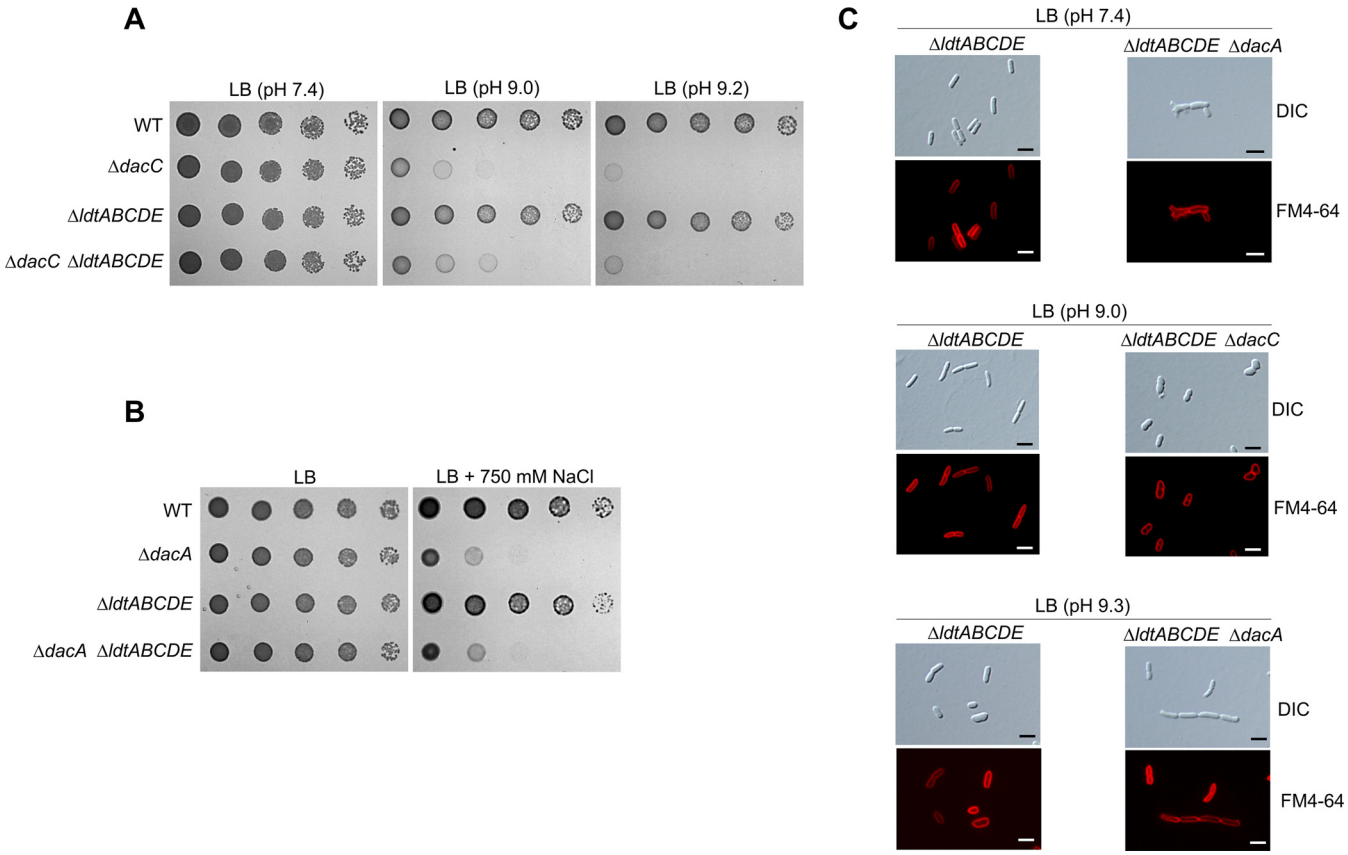

FIG 5 Identified phenotypes of the *dacC* and *dacA* mutants are independent of LD-transpeptidases. (A) LD-Transpeptidase-independent alkaline sensitivity of the *dacC* mutant. The wild-type (WT) and indicated mutant cells were serially diluted from 10^8 to 10^4 cells/mL in 10-fold steps and spotted onto an LB plate or LB plates at indicated pH. (B) LD-Transpeptidase-independent salt sensitivity of the *dacA* mutant. The wild-type and indicated mutant cells were serially diluted from 10^8 to 10^4 cells/mL in 10-fold steps and spotted onto an LB plate or an LB plate containing 750 mM NaCl. (C) LD-Transpeptidase-independent morphological changes of the *dacC* and *dacA* mutants. The indicated cells grown in LB medium or LB media at the indicated pH were stained with FM4-64 (red) and then spotted on a 1% agarose pad. Scale bars, 5 μm.

these interactions are also detected between DacC and PBPs, we performed pulldown experiments using DacC-Flag and DacC(ΔC)-Flag strains expressing His-tagged or nontagged PBPs. Despite similar intracellular expression levels of DacC, DacC was pulled down by His-tagged PBP1a, PBP1b, PBP2, and PBP3, but not by nontagged PBPs (Fig. 8A), indicating physical interactions between DacC and PBPs. When the same experiment was performed using the DacC(ΔC)-Flag strain, DacC(ΔC) was not pulled down by His-tagged PBPs, except for PBP2 (Fig. 8A), despite the higher expression levels of DacC(ΔC) than those of DacC (Fig. 8A) and similar levels of His-tagged PBPs eluted from DacC-Flag and DacC(ΔC)-Flag strains (Fig. S6). These results indicate that the C-terminal domain of DacC is required for physical interactions with PBP1a, PBP1b, and PBP3. Under the same experimental conditions, DacA also interacted with PBP1a, PBP1b, PBP2, and PBP3, and its C-terminal domain was required for physical interactions with PBP1a, PBP1b, PBP2, and PBP3 (Fig. 8B; Fig. S7). Collectively, these data show that both DacC and DacA physically interact with PBP1a, PBP1b, PBP2, and PBP3 and that their C-terminal domains are necessary for most interactions with PBPs.

Because both DacC and DacA are necessary for overcoming alkaline stress (Fig. 1 and 3), we checked whether the physical interaction between PBP and DacC or DacA is retained under alkaline stress conditions. This question was addressed by pulldown experiments using overexpressed PBP1b and His-tagged DacC or DacA. Significant amounts of PBP1b were pulled down by His-tagged DacC and DacA at both pHs 8.0 and 9.0 (Fig. 8C). PBP1b was not pulled down by His-tagged DacC(ΔC) and DacA(ΔC) at boths pH 8.0 and 9.0 (Fig. S8A), although the levels of purified His-tagged DacC(ΔC)

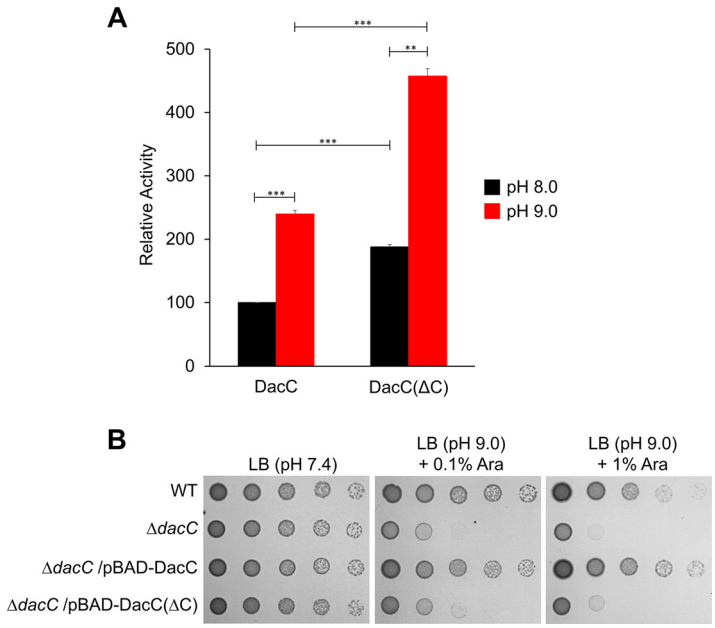

FIG 6 The C-terminal domain of DacC is necessary for bacterial growth under alkaline stress, but not its DD-CPase activity. (A) Enhanced DD-CPase activity of DacC(ΔC). The enzymatic activities of purified DacC and DacC(ΔC) were measured using the bacterial cell wall analog diacetyl-L-Lys–D-Ala–D-Ala (AcLAA). Purified proteins (1 μM) were incubated at 37°C with 50 mM Tris-HCl (pH 8.0 or 9.0) containing 1 mM AcLAA. The amount of released D-Ala was estimated using and Amplex Red and horseradish peroxidase at 563 nm. Data were obtained from three independent experiments. **, $P < 0.01$; ***, $P < 0.001$. (B) Requirement of the C-terminal domain of DacC for overcoming alkaline stress. The wild-type (WT) and indicated mutant cells were serially diluted from 10^8 to 10^4 cells/mL in 10-fold steps and spotted onto an LB plate or LB plate at pH 9.0 containing 0.1% or 1% arabinose.

and DacA(ΔC) were higher than those of purified His-tagged DacC and DacA, respectively (Fig. 8C; Fig. S8B). These results demonstrate the C-terminal domain-dependent interactions of DacC and DacA with PBP1b under alkaline stress conditions.

aPBPs are required for cell growth under stress conditions. The physical interactions of DacC and DacA with PBPs prompted us to investigate whether PBPs are required for bacterial growth at alkaline pH. Because PBP2 and PBP3 are essential (2), we measured the phenotype of the strain defective for PBP1a (encoded by the *mrcA* gene) or PBP1b (encoded by the *mrcB* gene). Notably, the *mrcB* mutant showed strong sensitivity to alkaline stress, whereas the *mrcA* mutant showed normal growth under alkaline stress conditions (Fig. 9A; Fig. S9A). Additionally, only the mutant defective in LpoB lipoprotein, an adaptor protein for the function of PBP1b, was also significantly sensitive to alkaline stress (Fig. 9A). These phenotypes were complemented by PBP1b or LpoB (Fig. 9B; Fig. S9B), indicating that PBP1b, but not PBP1a, is related to cell growth under alkaline stress. Given that PBP1b is an aPBP with both DD-transpeptidase and glycosyltransferase activities, we examined the activity of PBP1b involved in bacterial growth under alkaline stress. To address this question, we constructed two mutants: PBP1b(E233Q), defective in glycosyltransferase activity, and PBP1b(S510A), defective in DD-transpeptidase activity. Neither PBP1b(E233Q) nor PBP1b(S510A) complemented the phenotype of the *mrcB* mutant (Fig. 9C; Fig. S9C), indicating that both of these activities are involved in cell growth under alkaline stress. However, because the DD-transpeptidase activity of PBP1b is known to be dependent on glycosyltransferase activity (22, 39, 40), we cannot determine whether the result of PBP1b (E233Q) is caused by the loss of glycosyltransferase activity or by the glycosyltransferase defect-mediated loss of the DD-transpeptidase activity. Anyway, our results show that the DD-transpeptidase activity of PBP1b is required for cell growth under alkaline stress. A previous result showed that both PBP1a and PBP1b are required for bacterial growth under salt stress (18). Overall, these results indicate that the mutants defective for aPBPs phenocopy the *dacC* or *dacA* mutant.

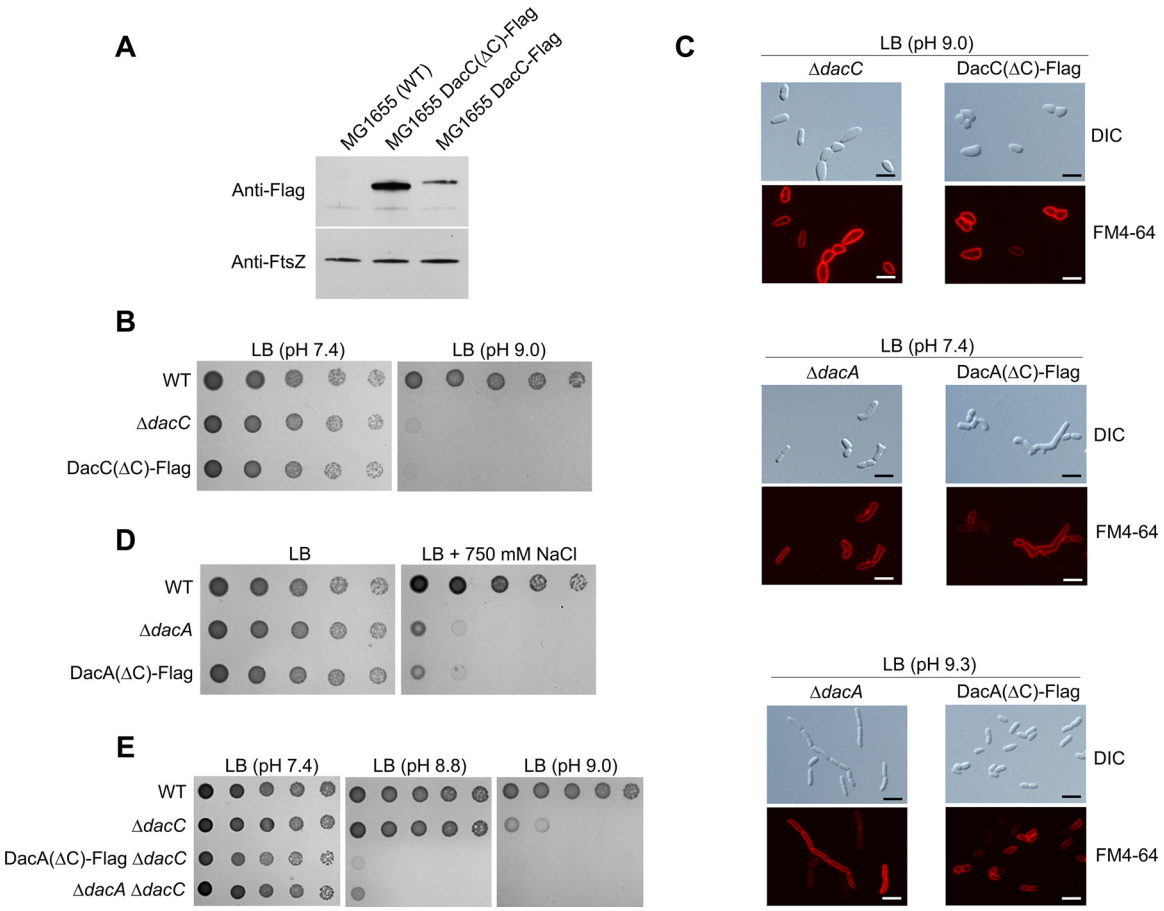

FIG 7 Phenotypes of the MG1655 DacC(ΔC)-Flag and MG1655 DacA(ΔC)-Flag strains. (A) Intracellular protein levels of DacC and DacC(ΔC). Western blot analysis with anti-Flag and anti-FtsZ antibodies was performed using 5×10^7 cells of indicated strains grown in LB medium to the early exponential phase (OD_{600} = 0.4). FtsZ was used as the loading control. (B) Sensitivity of the MG1655 DacC(ΔC)-Flag strain to alkaline pH. The wild-type (WT) and indicated mutant cells were serially diluted from 10^8 to 10^4 cells/mL in 10-fold steps and spotted onto an LB plate or LB plate at pH 9.0. (C) Morphological changes of the MG1655 DacC(ΔC)-Flag and MG1655 DacA(ΔC)-Flag strains. The indicated cells grown in LB medium or LB media at the indicated pH were stained with FM4-64 (red) and then spotted onto a 1% agarose pad. Scale bars, 5 μm. (D) Salt sensitivity of the MG1655 DacA(ΔC)-Flag strain. The wild-type and indicated mutant cells were serially diluted from 10^8 to 10^4 cells/mL in 10-fold steps and spotted onto an LB plate or LB plate containing 750 mM NaCl. (E) Phenotype of the MG1655 DacA(ΔC)-Flag Δ*dacC* strain under alkaline stress conditions. The wild-type and indicated mutant cells were serially diluted from 10^8 to 10^4 cells/mL in 10-fold steps and spotted onto an LB plate or LB plates at the indicated pH.

Because the deletion of aPBP does not induce any morphological change (2, 41), the morphological change in the *dacA* or *dacC* mutant may be related to PBP2 and PBP3. However, the shape of the *dacA* mutant in LB medium was different from both the spherical shape caused by inhibition of PBP2 and the filamentous shape caused by inhibition of PBP3 (2, 22). As DacA interacts with both PBP2 and PBP3, the morphological change in the *dacA* mutant may be associated with both PBP2 and PBP3. To address this question, we measured the morphological changes in the presence of amdinocillin (mecillinam) and aztreonam. MG1655 cells showed spherical or filamentous shapes in the presence of amdinocillin or aztreonam, respectively, whereas in the presence of a combination of amdinocillin and aztreonam, they showed a branched filamentous shape, which is similar to the shape of the *dacA* mutant (Fig. 9D), implying that the morphological change in the *dacA* mutant under normal conditions may be associated with both PBP2 and PBP3. The morphology of the *dacC* mutant under alkaline stress conditions significantly resembled a spherical shape upon inhibition of PBP2 (Fig. 4 and Fig. 9D). Therefore, these results imply that the morphological change in the *dacA* or *dacC* mutant may be related to bPBP.

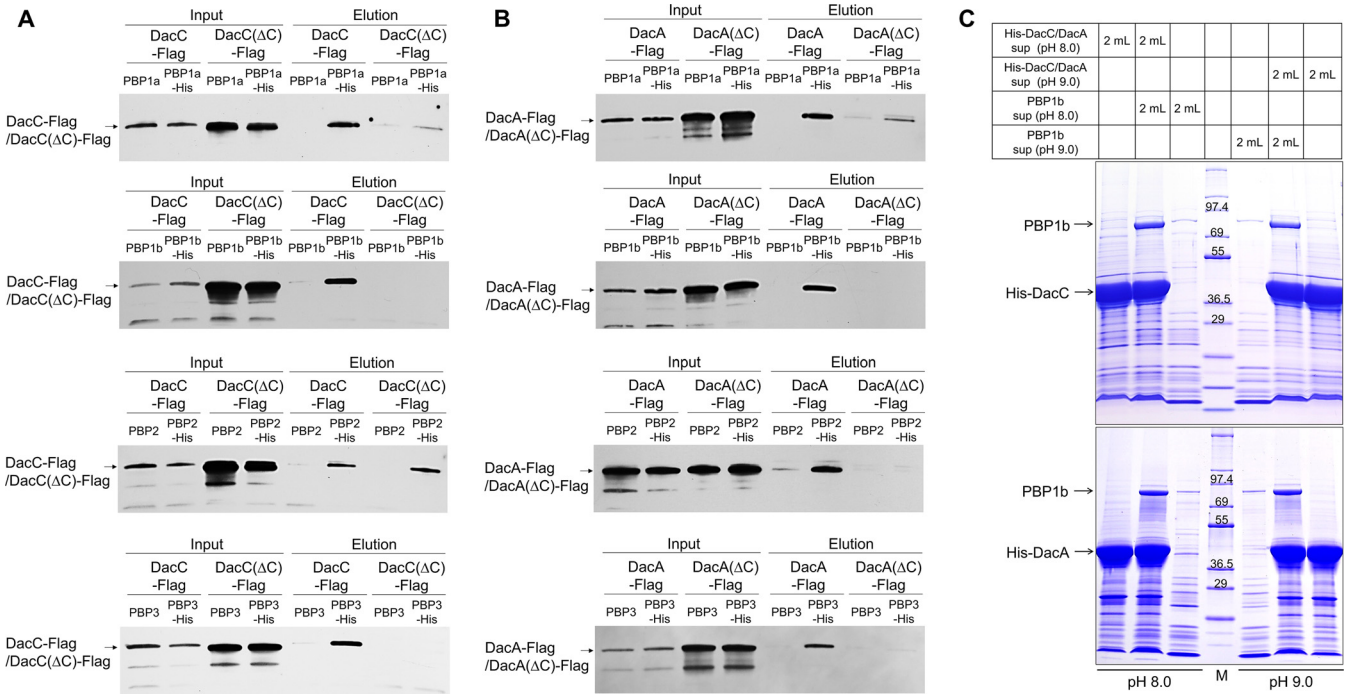

FIG 8 Physical interactions between PBPs and DacC or DacA. (A) C-terminal domain-dependent or -independent interactions of DacC with PBPs. The supernatant of MG1655 DacC-Flag or DacC(ΔC)-Flag cells harboring the pBAD-based plasmids expressing C-terminal His-tagged PBPs or nontagged PBPs was loaded onto Talon metal affinity resin. After pulldown experiments, the amounts of input (Input) and output (Elution) DacC or DacC(ΔC) were measured by Western blotting using monoclonal antibody against Flag tag. (B) C-terminal domain-dependent interactions of DacA with PBPs. The supernatant of MG1655 DacA-Flag or DacA(ΔC)-Flag cells harboring the pBAD-based plasmids expressing C-terminal His-tagged PBPs or nontagged PBPs was loaded onto Talon metal affinity resin. After pulldown experiments, the amounts of input (Input) and output (Elution) DacA or DacA(ΔC) were measured by Western blotting using monoclonal antibody against Flag tag. (C) Physical interaction between PBP1b and DacC or DacA under alkaline stress conditions. The supernatant of ER2566 cells harboring the pET24a plasmid expressing PBP1b was mixed with the supernatant of ER2566 cells harboring pET28a plasmid expressing His-tagged DacC or His-tagged DacA at pH 8.0 or 9.0. After pulldown experiments, eluted proteins were separated on 4 to 20% gradient Tris-glycine polyacrylamide gels and visualized by staining with Coomassie brilliant blue R. Lane M contains the EzWay Protein Blue MW marker (KOMA Biotech).

DISCUSSION

PG degradation and modification by PG hydrolases play a pivotal role in bacterial physiology, such as morphology and adaptation to environmental stresses. Among PG hydrolases, the physiological function of DD-CPases controlling the amount of pentapeptide substrates is poorly understood. In this study, we demonstrated that DD-CPases DacA and DacC are necessary for shape maintenance and cell growth under environmental stresses. DacA and DacC interacted with both aPBP and bPBP, mostly in a C-terminal domain-dependent manner, and these interactions were required for most of their functions in shape maintenance and cell growth under environmental stresses. Notably, these roles of DacA and DacC were not dependent on LD-transpeptidases. These results demonstrate that DacA and DacC play LD-transpeptidase-independent physiological roles in shape maintenance and bacterial growth under stress conditions, which may be associated with physical interactions with PBPs.

We found that DacA and DacC play coordinated and distinct roles in cell growth and shape maintenance under stress conditions. Both DacC and DacA were required to overcome alkaline stress, whereas only DacA was required to overcome salt stress (Fig. 3; see Fig. S1 in the supplemental material). Both DacA and DacC were necessary for morphological maintenance, but their effects were distinct. Under normal conditions, loss of DacA induced aberrant cell morphology, whereas loss of DacC hardly affected cell morphology (Fig. 4). Under alkaline stress conditions, loss of DacA induced a filamentous shape, whereas loss of DacC induced a spherical shape (Fig. 4). Because inhibition of PBP2 results in the spherical shape and inhibition of PBP3 causes the filamentous shape (2, 22), distinct morphological changes of the *dacC* and *dacA* mutants under alkaline stress conditions could be

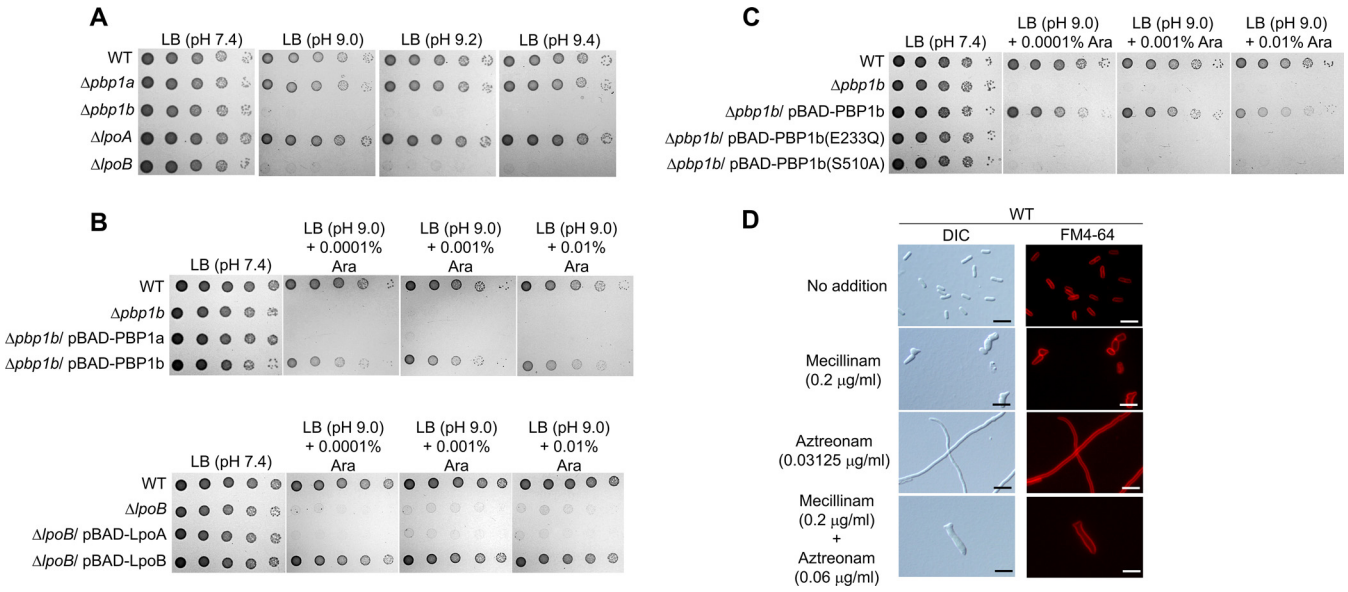

FIG 9 aPBP is required for cell growth under alkaline stress. (A) Sensitivity of *mrcB* and *lpoB* mutants to alkaline stress. The wild-type (WT) and indicated mutant cells were serially diluted from 10^8 to 10^4 cells/mL in 10-fold steps and spotted onto an LB plate or LB plates at the indicated pH. (B) Complementation of alkaline sensitivity of *mrcB* and *lpoB* mutants. The cells of the indicated strains were serially diluted from 10^8 to 10^4 cells/mL in 10-fold steps and spotted onto an LB plate and LB plates at pH 9.0 containing the indicated concentrations of arabinose. (C) Requirement of the DD-transpeptidase activity of PBP1b for overcoming alkaline stress. The cells of the indicated strains were serially diluted from 10^8 to 10^4 cells/mL in 10-fold steps and spotted onto an LB plate or LB plates at pH 9.0 containing the indicated concentrations of arabinose. (D) Effect of PBP2 or/and PBP3 inhibition on bacterial morphology. The MG1655 cells grown in LB media containing the indicated concentrations of amdinocillin (mecillinam) or/and aztreonam were stained with FM4-64 (red) and then spotted onto a 1% agarose pad. Scale bars, 5 μm.

associated with the functional defects of PBP2 and PBP3, respectively. Basically, these distinct functions of DacA and DacC appear to be based on their protein levels. DacC is an alkaline DD-CPase, whose stability and activity are significantly increased under alkaline stress conditions (Fig. 2). Therefore, in LB medium, only DacA appears to play a predominant role in shape maintenance and cell growth. DacD, on the other hand, plays only a minor role in LB medium, consistent with a previous study showing that the stability and activity of this DD-CPase are increased under acidic conditions (21). To date, we do not know why DacA and DacC show distinct morphological effects under alkaline stress conditions.

PG hydrolases and periplasmic proteins participating in PG synthesis exhibit high functional redundancy (more than 36 enzymes for 9 reactions) (22, 42). Recent studies demonstrated that several periplasmic enzymes play an important role under specific stress conditions (10, 18, 21, 22). AmiB and DacD were identified as acid-specific PG amidase and carboxypeptidase, respectively, which play a physiological role under acid stress (10, 21). PBP1b was identified as an acid-tolerant aPBP that retains its enzymatic activity under acid stress and is required for bacterial growth under acid stress (22). Among PG endopeptidases, MepM and MepS are required for bacterial growth under salt and EDTA stresses, respectively (18). In this study, we identified that DacC is a DD-CPase that is specialized for bacterial growth under alkaline stress. Because the periplasm is a space that is sensitive to diverse extracellular harsh perturbations (22, 43), other periplasmic enzymes thus seem to be participating in overcoming specific periplasmic stress conditions.

We demonstrated that DacA, DacC, and PBP1b are required to overcome alkaline stress (Fig. 3 and 9). Although PBP1b was dispensable for growth under weak alkaline stress conditions (22), it was obligately necessary for growth under strong alkaline stress conditions (Fig. 9). *E. coli* encounters strong alkaline stress conditions exceeding pH 10 at the pancreatic duct (44, 45). Alkaline stress is known to strongly induce a CpxAR two-component system that senses envelope stress (46–48), but the molecular mechanism by which alkaline stress induces the CpxAR system has not been elucidated. As our results imply that alkaline stress might affect PG synthesis or stability, the effect of alkaline stress on PG should be analyzed in further studies.

All DD-CPase-mediated phenotypes identified in this study were independent of LD-transpeptidases. In the absence of all LD-transpeptidases, all phenotypes of the *dacA* and *dacC* mutants were observed (Fig. 5). The C-terminal domain of DacC was dispensable for its enzymatic activity but was required for complementation of all phenotypes of the *dacC* mutant and physical interactions with PBPs, except for PBP2. The C-terminal domain of DacA is dispensable for its enzymatic activity (32), but was required for complementation of all phenotypes of the *dacA* mutant, except for filamentous morphology under alkaline stress, and all physical interactions with PBPs. These results suggest that many functions of DacA and DacC are not linked to LD-transpeptidase, but instead they may be associated with DD-transpeptidases PBPs, through interactions involving the C-terminal domain of DD-CPases. At present, we do not know how DacA and DacC affect the functions of PBPs or act cooperatively in PG synthesis with PBPs. We previously reported divergent phenotypes of the *dacA* mutant toward antibiotics, vancomycin resistance, and β-lactam sensitivity (32). The β-lactam sensitivity of the *dacA* mutant was dependent on the C-terminal domain of DacA, whereas vancomycin resistance was independent of its C-terminal domain (32), like filamentous morphology under alkaline stress in this study. These results indicate that the cellular functions of DacA are more diverse than expected. Based on the phenotypes of PBP-defective mutants, we predicted which PBPs were associated with the phenotypes of the *dacC* and *dacA* mutants. aPBPs appear to be involved in cell growth under alkaline and salt stresses (18) (Fig. 9). These results are consistent with a previous study showing that aPBPs contribute to PG repair rather than to morphological maintenance (41). Further studies are required to elucidate the interactions with PBPs that are linked to the physiological roles of DacA and DacC.

MATERIALS AND METHODS

Bacterial strains, plasmids, and culture conditions. All *E. coli* strains and plasmids used in this study are listed in Table S1 in the supplemental material, and all primer sequences used in this study are presented in Table S2. All cells were cultured in LB medium (tryptone, 10 g/L; yeast extract, 5 g/L; sodium chloride, 10 g/L) at 37°C, unless otherwise stated. Ampicillin (100 μg/mL), kanamycin (50 μg/mL), chloramphenicol (5 μg/mL), and tetracycline (10 μg/mL) were added into the culture medium, when necessary. Alkaline LB medium was prepared by adding 50 mM Tris (final concentration), followed by pH adjustment of the medium using 10 N NaOH solution. The final pH of medium was defined as the pH of medium after an autoclave sterilization process, due to the slight decrease of pH after the autoclave process.

All deletion strains were constructed using the plasmid pKD46 expressing λ red recombinase, as previously described (49), with some modifications. Deletion cassettes for the exchange of the target gene with the FLP recombination target (FRT) sequence containing the kanamycin resistance gene were amplified from the pKD13 plasmid. After PCR purification, deletion cassettes were transformed into MG1655 cells harboring the pKD46 plasmid. Transformed cells were spread onto LB medium plates containing kanamycin, and plates were incubated at 37°C or 30°C overnight. The deletion strain was confirmed using PCR. To remove the kanamycin resistance gene, the pCP20 plasmid expressing FLP recombinase, which catalyzes recombination between FRT sequences, was transformed into the deletion strain. Removal of the kanamycin resistance gene was also confirmed using PCR. To minimize the impact on the physiology of the deletion strain, the pCP20 plasmid was removed at 37°C, as previously reported (18).

The insertion of a 3×Flag gene into the chromosomal 3′ region of the target gene was performed using λ red recombinase, as previously reported (32, 50). The plasmid pBAD-Flag-FRT-Kan, which contained both the 3×Flag gene and the FRT-flanked kanamycin resistance gene, was used as a template for PCR amplification using the primer sets listed in Table S2. After PCR amplification, the pBAD-Flag-FRT-Kan plasmid, which was used as a template, was removed by overnight treatment with the restriction enzyme DpnI. The insertion of both the 3×Flag gene and kanamycin resistance gene was conducted in the MG1655 strain harboring the pKD46 plasmid. After chromosomal fusion of the 3×Flag-tag, the kanamycin resistance gene was removed using the pCP20 plasmid expressing FLP recombinase, as described above. In the MG1655 DacC(ΔC)-Flag strain, the 3×Flag epitope was inserted at the 378th amino acid (glycine residue) of DacC instead of its C-terminal amino acid (serine residue).

To construct the pBAD-DacC plasmid, the region covering the entire open reading frame of the *dacC* gene was amplified. After PCR purification, the *dacC* gene was inserted into the pBAD24 plasmid digested with EcoRI and XbaI. The insertion was conducted by recombination of overlapping sequences using In-Fusion cloning (Clontech, USA), as previously reported (18). The cloning of the *dacC* gene was confirmed by sequence analysis. The plasmid pBAD-DacC(S66G) was constructed by PCR using pBAD-DacC as a template and DpnI-dependent digestion of the template plasmid. The other pBAD-based plasmids were constructed using the same method. The pET24a-based plasmids expressing nontagged WT proteins and pET28a-based plasmids expressing His-tagged proteins were constructed using similar methods, except the NdeI and BamHI restriction enzymes were used for plasmid digestion. pRE1-based

plasmids were constructed using similar methods, except the NdeI and XbaI restriction enzymes were used for plasmid digestion. Because the gene in the pRE1 plasmid is transcribed by *E. coli* RNA polymerase under the control of a combination of strong λ P_L promoter and cI ribosome binding site, it is constitutively transcribed in general *E. coli* strains without the cI protein, such as MG1655 (51, 52). The pACYC184-based plasmids were constructed using similar methods, except the BamHI and EagI restriction enzymes were used for plasmid digestion. In this study, the region covering both the promoter region and the entire open leading frame of the target gene was cloned into the pACYC184 plasmid. All of the primers used for plasmid construction are listed in Table S2.

Measurement of bacterial growth. Cells grown in LB medium overnight were inoculated into LB medium, and when the optical density at 600 nm (OD_{600}) reached ~1.0, the cells were diluted from 10^8 to 10^4 cells/mL in 10-fold dilutions. Aliquots of 2 μL were spotted onto LB plates, LB plates were adjusted to the indicated pH, or LB plates were supplemented with 750 mM NaCl. After 8 to 20 h of incubation at 37°C, photographs of the plates were taken with an EOS 100D digital camera (Canon, Inc., Japan). All bacterial growth results were determined from three independent experiments.

Quantitative real-time PCR. To measure the mRNA level of *dacC* at high pH, total RNA was extracted from the cells cultured in LB medium or LB medium buffered to pH 9.0. Total RNA was extracted when the cells reached an OD_{600} of ~0.4. To remove genomic DNA, each RNA sample was incubated with RNase-free DNase I (Promega, USA) at 37°C for 1 h. The remaining RNA was converted into cDNAs using the cDNA EcoDry premix (Clontech, USA). Quantitative real-time PCR was performed using 10-fold-diluted cDNAs as the template. Primers for the detection of *dacC* or 16S rRNA listed in Table S2 were used, and amplification was performed using the SYBR Premix *Ex Taq* II (TaKaRa, Japan) solution. PCR and simultaneous fluorescence detection were performed using a CFX96 real-time System (Bio-Rad, USA). The expression level of *dacC* was calculated as the difference between the threshold cycle of *dacC* and that of the 16S rRNA reference gene.

Detection of intracellular levels of DD-CPases. The protein levels of DacA, DacC, and DacD were detected using MG1655 strains with chromosomal insertion of the 3×Flag gene into the 3′ region of each gene. The cells were cultured in LB medium or LB medium buffered to pH 9.0 or 9.2 and were harvested at an OD_{600} of ~0.4. After the addition of sodium dodecyl sulfate sample buffer, the samples were boiled at 100°C for 5 min. Total proteins were separated on 4 to 20% Tris–glycine polyacrylamide gels (KOMA Biotech, South Korea) and were transferred onto polyvinylidene difluoride (PVDF) membranes. The protein levels of DD-CPases and DnaK were determined using monoclonal antibodies against Flag tag (Santa Cruz Biotechnology, USA) and anti-DnaK (Abcam, USA), respectively, according to the standard procedures. DnaK was used as a loading control. The protein level of DacC(ΔC) was detected using similar procedures, except that FtsZ was used as a loading control.

Measurement of protein stability of DacC. Protein stability of DacC was measured in LB medium and LB medium buffered to pH 9.0. The MG1655 DacC-Flag strain was cultured to an OD_{600} of ~0.4. After addition of spectinomycin (200 μg/mL), 6×10^7 cells were harvested at 10, 20, and 40 min. The protein level of DacC was detected using a monoclonal antibody against the Flag tag (Santa Cruz Biotechnology), according to the Western blot protocol described above.

Purification of DD-CPase proteins. ER2566 cells harboring the pET28a-based plasmid expressing His-tagged DacC or DacC(ΔC) were cultured in LB medium at 37°C. When the OD_{600} was ~0.5, 1 mM isopropyl-β-D-1-thiogalactopyranoside (IPTG) was added to 200 mL of LB medium and cells were cultured at 16°C overnight. Harvested cells were suspended in 3 mL of binding buffer (50 mM Tris-HCl [pH 8.0], 200 mM NaCl, and 1% sodium *n*-dodecyl-β-D-maltoside) and disrupted twice using a French press at 10,000 lb/in^2. The disrupted cells were separated by centrifugation at 9,000 × *g* for 30 min at 4°C, and the supernatant was loaded into 0.5 mL of a Talon metal affinity resin (Clontech) equilibrated with binding buffer. After washing the resin with 3 mL of binding buffer three times, the bound proteins were eluted using elution buffer (50 mM Tris-HCl [pH 8.0], 150 mM NaCl, 200 mM imidazole). To remove imidazole, the eluted samples were dialyzed with 3 L dialysis buffer (50 mM Tris-HCl [pH 8.0], 50 mM NaCl). The purified proteins were promptly used to assess the enzymatic activity of DD-CPases.

Assessment of the enzymatic activity of DD-CPases. The enzymatic activity of purified His-tagged DacC or DacC(ΔC) was measured using the bacterial cell wall analog diacetyl-L-Lys–D-Ala–D-Ala (AcLAA) (21). D-Ala released by DacC or DacC(ΔC) was degraded into hydrogen peroxide, pyruvate, and amine group by D-amino acid oxidase (Sigma-Aldrich). Hydrogen peroxide was reduced to H_2O by horseradish peroxidase (Sigma-Aldrich) using Amplex Red (Invitrogen, USA) as the electron donor. Then, Amplex Red was converted to resorufin by oxidation, and the amount of resorufin was spectrophotometrically measured at 563 nm. The purified His-tagged DacC or DacC(ΔC) protein (1 μM) was mixed with 50 mM Tris-HCl (pH 8.0 or 9.0) containing 1 mM AcLAA in a final volume of 200 μL. After incubation for 60 min at 37°C, the enzymatic reaction was halted by boiling at 100°C for 20 min. The samples were centrifuged at 13,000 rpm for 5 min, and the supernatant was transferred to 800 μL of assay buffer containing 50 mM HEPES-NaOH (pH 7.5), 50 μM Amplex Red, 75 μg/mL D-amino acid oxidase, 54 μg/mL horseradish peroxidase, and 10 mM $MgCl_2$. After incubation at 37°C for 60 min, the amount of resorufin was measured at 563 nm using a UVmini-1240 UV-visible (UV-Vis) spectrophotometer (Shimadzu, Japan).

Detection of the physical interaction of DD-CPases with PBPs. Physical interactions between DD-CPases and PBPs (PBP1a, PBP1b, PBP2, and PBP3) were detected through pulldown experiments. To perform the pulldown assay, we constructed pBAD-based plasmids expressing C-terminal His-tagged PBPs or nontagged PBPs. These plasmids were transformed into the MG1655 chromosomal DacC-Flag, DacC(ΔC)-Flag, DacA-Flag, and DacA(ΔC)-Flag strains. The strains were cultured in LB medium at 37°C to an OD_{600} of ~0.5. After addition of 1% arabinose, the cells were cultured at 30°C for 3 h. Harvested cells were suspended in 3 mL of binding buffer without 1% sodium *n*-dodecyl-β-D-maltoside and were

disrupted twice by a French press at 10,000 lb/in^2. After centrifugation at 9,000 $\times$ *g* for 10 min at 4°C, the supernatant was mixed with 0.5 mL of the Talon metal affinity resin. After washing the resin three times, the bound proteins were eluted using elution buffer. Total proteins were separated on 4 to 20% Tris–glycine polyacrylamide gels (KOMA Biotech) and were transferred onto PVDF membranes. The protein levels of DacC, DacC(ΔC), DacA, and DacA(ΔC) were determined using a monoclonal antibody against Flag tag (Santa Cruz Biotechnology), according to the standard procedure.

To analyze the effect of alkaline pH on the physical interactions between DD-CPases and PBP1b, ER2566 strains harboring the pET-based plasmids expressing His-tagged DacC, His-tagged DacA, or non-tagged PBP1b were cultured in 100 mL of LB medium at 37°C. When the OD_{600} was ~0.5, 1 mM IPTG was added to medium, and then the cells were cultured at 16°C overnight. Harvested cells were suspended in 4.5 mL of binding buffer at pH 8.0 or 9.0, as described above, and were disrupted twice by a French press at 10,000 lb/in^2. After centrifugation at 9,000 $\times$ *g* for 30 min at 4°C, only the supernatant was mixed with 100 μL of the Talon metal affinity resin in a 1.5-mL tube. After gentle rotation at 4°C and centrifugation at 7,000 rpm for 30 s, the supernatant was deliberately removed. Proteins were bound to the resin by repeated mixing, rotation, centrifugation, and supernatant removal. The resin was washed more than five times with 1 mL binding buffer at pH 8.0 or 9.0. The bound proteins were eluted with elution buffer containing 200 mM imidazole and were separated on 4 to 20% gradient Tris-glycine polyacrylamide gels (KOMA Biotech). The separated proteins were visualized by staining with Coomassie brilliant blue R.

Evaluation of cell shape using microscopy. The cells were cultured at 37°C in LB medium at various pHs with or without 0.2% arabinose or antibiotics. At an OD_{600} of ~0.4, the cells were stained with 5 μg/mL FM4-64 [N-(3-triethylammoniumpropyl)-4-(*p*-diethylaminophenylhexatrienyl)-pyridinium dibromide] for 10 min at room temperature and spotted on a 1% agarose pad prepared in phosphate-buffered saline. The cells were visualized under an Eclipse Ni microscope (Nikon, Japan).

SUPPLEMENTAL MATERIAL

Supplemental material is available online only.

SUPPLEMENTAL FILE 1, PDF file, 1.6 MB.

ACKNOWLEDGMENTS

This work was supported by research grants from Basic Science Research Program through the National Research Foundation of Korea funded by the Ministry of Education (NRF-2020R1I1A2058026, 2021R1A6A3A01086677, and 2021R1A6A3A01086629) and Korea Institute of Planning and Evaluation for Technology in Food, Agriculture and Forestry (IPET) through the High Value-added Food Technology Development Program, funded by the Ministry of Agriculture, Food and Rural Affairs (MAFRA) (grant no. 322026-3).

REFERENCES

1. Vollmer W, Bertsche U. 2008. Murein (peptidoglycan) structure, architecture and biosynthesis in *Escherichia coli*. Biochim Biophys Acta 1778:1714–1734. https://doi.org/10.1016/j.bbamem.2007.06.007.
2. Rohs PDA, Bernhardt TG. 2021. Growth and division of the peptidoglycan matrix. Annu Rev Microbiol 75:315–336. https://doi.org/10.1146/annurev-micro-020518-120056.
3. Dorr T. 2021. Understanding tolerance to cell wall-active antibiotics. Ann N Y Acad Sci 1496:35–58. https://doi.org/10.1111/nyas.14541.
4. Hugonnet JE, Mengin-Lecreulx D, Monton A, den Blaauwen T, Carbonnelle E, Veckerle C, Brun YV, van Nieuwenhze M, Bouchier C, Tu K, Rice LB, Arthur M. 2016. Factors essential for L,D-transpeptidase-mediated peptidoglycan cross-linking and β-lactam resistance in *Escherichia coli*. eLife 5:e19469. https://doi.org/10.7554/eLife.19469.
5. Baranowski C, Welsh MA, Sham LT, Eskandarian HA, Lim HC, Kieser KJ, Wagner JC, McKinney JD, Fantner GE, Ioerger TR, Walker S, Bernhardt TG, Rubin EJ, Rego EH. 2018. Maturing *Mycobacterium smegmatis* peptidoglycan requires non-canonical crosslinks to maintain shape. eLife 7:e37516. https://doi.org/10.7554/eLife.37516.
6. van Heijenoort J. 2011. Peptidoglycan hydrolases of *Escherichia coli*. Microbiol Mol Biol Rev 75:636–663. https://doi.org/10.1128/MMBR.00022-11.
7. Vermassen A, Leroy S, Talon R, Provot C, Popowska M, Desvaux M. 2019. Cell wall hydrolases in bacteria: insight on the diversity of cell wall amidases, glycosidases and peptidases toward peptidoglycan. Front Microbiol 10:331. https://doi.org/10.3389/fmicb.2019.00331.
8. Vollmer W, Joris B, Charlier P, Foster S. 2008. Bacterial peptidoglycan (murein) hydrolases. FEMS Microbiol Rev 32:259–286. https://doi.org/10.1111/j.1574-6976.2007.00099.x.
9. Uehara T, Parzych KR, Dinh T, Bernhardt TG. 2010. Daughter cell separation is controlled by cytokinetic ring-activated cell wall hydrolysis. EMBO J 29:1412–1422. https://doi.org/10.1038/emboj.2010.36.
10. Mueller EA, Iken AG, Ali Ozturk M, Winkle M, Schmitz M, Vollmer W, Di Ventura B, Levin PA. 2021. The active repertoire of *Escherichia coli* peptidoglycan amidases varies with physiochemical environment. Mol Microbiol 116:311–328. https://doi.org/10.1111/mmi.14711.
11. Cho H, Uehara T, Bernhardt TG. 2014. Beta-lactam antibiotics induce a lethal malfunctioning of the bacterial cell wall synthesis machinery. Cell 159:1300–1311. https://doi.org/10.1016/j.cell.2014.11.017.
12. Yunck R, Cho H, Bernhardt TG. 2016. Identification of MltG as a potential terminase for peptidoglycan polymerization in bacteria. Mol Microbiol 99:700–718. https://doi.org/10.1111/mmi.13258.
13. Bohrhunter JL, Rohs PDA, Torres G, Yunck R, Bernhardt TG. 2021. MltG activity antagonizes cell wall synthesis by both types of peptidoglycan polymerases in *Escherichia coli*. Mol Microbiol 115:1170–1180. https://doi.org/10.1111/mmi.14660.
14. Sassine J, Pazos M, Breukink E, Vollmer W. 2021. Lytic transglycosylase MltG cleaves in nascent peptidoglycan and produces short glycan strands. Cell Surf 7:100053. https://doi.org/10.1016/j.tcsw.2021.100053.
15. Nambu T, Minamino T, Macnab RM, Kutsukake K. 1999. Peptidoglycan-hydrolyzing activity of the FlgJ protein, essential for flagellar rod formation in *Salmonella typhimurium*. J Bacteriol 181:1555–1561. https://doi.org/10.1128/JB.181.5.1555-1561.1999.
16. Santin YG, Cascales E. 2017. Domestication of a housekeeping transglycosylase for assembly of a type VI secretion system. EMBO Rep 18:138–149. https://doi.org/10.15252/embr.201643206.
17. Lai GC, Cho H, Bernhardt TG. 2017. The mecillinam resistome reveals a role for peptidoglycan endopeptidases in stimulating cell wall synthesis

in *Escherichia coli*. PLoS Genet 13:e1006934. https://doi.org/10.1371/journal.pgen.1006934.
18. Park SH, Kim YJ, Lee HB, Seok YJ, Lee CR. 2020. Genetic evidence for distinct functions of peptidoglycan endopeptidases in *Escherichia coli*. Front Microbiol 11:565767. https://doi.org/10.3389/fmicb.2020.565767.
19. Singh SK, SaiSree L, Amrutha RN, Reddy M. 2012. Three redundant murein endopeptidases catalyse an essential cleavage step in peptidoglycan synthesis of *Escherichia coli* K12. Mol Microbiol 86:1036–1051. https://doi.org/10.1111/mmi.12058.
20. Chodisetti PK, Reddy M. 2019. Peptidoglycan hydrolase of an unusual cross-link cleavage specificity contributes to bacterial cell wall synthesis. Proc Natl Acad Sci U S A 116:7825–7830. https://doi.org/10.1073/pnas.1816893116.
21. Peters K, Kannan S, Rao VA, Biboy J, Vollmer D, Erickson SW, Lewis RJ, Young KD, Vollmer W. 2016. The redundancy of peptidoglycan carboxypeptidases ensures robust cell shape maintenance in *Escherichia coli*. mBio 7:e00819-16. https://doi.org/10.1128/mBio.00819-16.
22. Mueller EA, Egan AJ, Breukink E, Vollmer W, Levin PA. 2019. Plasticity of *Escherichia coli* cell wall metabolism promotes fitness and antibiotic resistance across environmental conditions. eLife 8:e40754. https://doi.org/10.7554/eLife.40754.
23. Buchanan CE, Sowell MO. 1982. Synthesis of penicillin-binding protein 6 by stationary-phase *Escherichia coli*. J Bacteriol 151:491–494. https://doi.org/10.1128/jb.151.1.491-494.1982.
24. Li GW, Burkhardt D, Gross C, Weissman JS. 2014. Quantifying absolute protein synthesis rates reveals principles underlying allocation of cellular resources. Cell 157:624–635. https://doi.org/10.1016/j.cell.2014.02.033.
25. Nelson DE, Young KD. 2000. Penicillin binding protein 5 affects cell diameter, contour, and morphology of *Escherichia coli*. J Bacteriol 182:1714–1721. https://doi.org/10.1128/JB.182.6.1714-1721.2000.
26. Ghosh AS, Young KD. 2003. Sequences near the active site in chimeric penicillin binding proteins 5 and 6 affect uniform morphology of *Escherichia coli*. J Bacteriol 185:2178–2186. https://doi.org/10.1128/JB.185.7.2178-2186.2003.
27. More N, Martorana AM, Biboy J, Otten C, Winkle M, Serrano CKG, Monton Silva A, Atkinson L, Yau H, Breukink E, den Blaauwen T, Vollmer W, Polissi A. 2019. Peptidoglycan remodeling enables *Escherichia coli* to survive severe outer membrane assembly defect. mBio 10:e02729-18. https://doi.org/10.1128/mBio.02729-18.
28. Baquero MR, Bouzon M, Quintela JC, Ayala JA, Moreno F. 1996. *dacD*, an *Escherichia coli* gene encoding a novel penicillin-binding protein (PBP6b) with DD-carboxypeptidase activity. J Bacteriol 178:7106–7111. https://doi.org/10.1128/jb.178.24.7106-7111.1996.
29. O'Daniel PI, Zajicek J, Zhang W, Shi Q, Fisher JF, Mobashery S. 2010. Elucidation of the structure of the membrane anchor of penicillin-binding protein 5 of *Escherichia coli*. J Am Chem Soc 132:4110–4118. https://doi.org/10.1021/ja9094445.
30. Nelson DE, Ghosh AS, Paulson AL, Young KD. 2002. Contribution of membrane-binding and enzymatic domains of penicillin binding protein 5 to maintenance of uniform cellular morphology of *Escherichia coli*. J Bacteriol 184:3630–3639. https://doi.org/10.1128/JB.184.13.3630-3639.2002.
31. Potluri L, Karczmarek A, Verheul J, Piette A, Wilkin JM, Werth N, Banzhaf M, Vollmer W, Young KD, Nguyen-Disteche M, den Blaauwen T. 2010. Septal and lateral wall localization of PBP5, the major D,D-carboxypeptidase of *Escherichia coli*, requires substrate recognition and membrane attachment. Mol Microbiol 77:300–323. https://doi.org/10.1111/j.1365-2958.2010.07205.x.
32. Park SH, Choi U, Ryu SH, Lee HB, Lee JW, Lee CR. 2022. Divergent effects of peptidoglycan carboxypeptidase DacA on intrinsic β-lactam and vancomycin resistance. Microbiol Spectr 10:e01734-22. https://doi.org/10.1128/spectrum.01734-22.
33. Sarkar SK, Chowdhury C, Ghosh AS. 2010. Deletion of penicillin-binding protein 5 (PBP5) sensitises *Escherichia coli* cells to β-lactam agents. Int J Antimicrob Agents 35:244–249. https://doi.org/10.1016/j.ijantimicag.2009.11.004.
34. Nelson DE, Young KD. 2001. Contributions of PBP5 and DD-carboxypeptidase penicillin binding proteins to maintenance of cell shape in *Escherichia coli*. J Bacteriol 183:3055–3064. https://doi.org/10.1128/JB.183.10.3055-3064.2001.
35. Winkle M, Hernandez-Rocamora VM, Pullela K, Goodall ECA, Martorana AM, Gray J, Henderson IR, Polissi A, Vollmer W. 2021. DpaA detaches Braun's lipoprotein from peptidoglycan. mBio 12:e00836-21. https://doi.org/10.1128/mBio.00836-21.
36. Bahadur R, Chodisetti PK, Reddy M. 2021. Cleavage of Braun's lipoprotein Lpp from the bacterial peptidoglycan by a paralog of L,D-transpeptidases, LdtF. Proc Natl Acad Sci U S A 118:e2101989118. https://doi.org/10.1073/pnas.2101989118.
37. Harris F, Brandenburg K, Seydel U, Phoenix D. 2002. Investigations into the mechanisms used by the C-terminal anchors of *Escherichia coli* penicillin-binding proteins 4, 5, 6 and 6b for membrane interaction. Eur J Biochem 269:5821–5829. https://doi.org/10.1046/j.1432-1033.2002.03295.x.
38. van der Linden MP, de Haan L, Hoyer MA, Keck W. 1992. Possible role of *Escherichia coli* penicillin-binding protein 6 in stabilization of stationary-phase peptidoglycan. J Bacteriol 174:7572–7578. https://doi.org/10.1128/jb.174.23.7572-7578.1992.
39. Egan AJ, Jean NL, Koumoutsi A, Bougault CM, Biboy J, Sassine J, Solovyova AS, Breukink E, Typas A, Vollmer W, Simorre JP. 2014. Outer-membrane lipoprotein LpoB spans the periplasm to stimulate the peptidoglycan synthase PBP1B. Proc Natl Acad Sci U S A 111:8197–8202. https://doi.org/10.1073/pnas.1400376111.
40. Bertsche U, Breukink E, Kast T, Vollmer W. 2005. In vitro murein peptidoglycan synthesis by dimers of the bifunctional transglycosylase-transpeptidase PBP1B from *Escherichia coli*. J Biol Chem 280:38096–38101. https://doi.org/10.1074/jbc.M508646200.
41. Vigouroux A, Cordier B, Aristov A, Alvarez L, Ozbaykal G, Chaze T, Oldewurtel ER, Matondo M, Cava F, Bikard D, van Teeffelen S. 2020. Class-A penicillin binding proteins do not contribute to cell shape but repair cell-wall defects. eLife 9:e51998. https://doi.org/10.7554/eLife.51998.
42. Pazos M, Peters K, Vollmer W. 2017. Robust peptidoglycan growth by dynamic and variable multi-protein complexes. Curr Opin Microbiol 36:55–61. https://doi.org/10.1016/j.mib.2017.01.006.
43. Rosenbusch JP. 1990. Structural and functional properties of porin channels in *E. coli* outer membranes. Experientia 46:167–173.
44. Padan E, Bibi E, Ito M, Krulwich TA. 2005. Alkaline pH homeostasis in bacteria: new insights. Biochim Biophys Acta 1717:67–88. https://doi.org/10.1016/j.bbamem.2005.09.010.
45. Hamdallah I, Torok N, Bischof KM, Majdalani N, Chadalavada S, Mdluli N, Creamer KE, Clark M, Holdener C, Basting PJ, Gottesman S, Slonczewski JL. 2018. Experimental evolution of *Escherichia coli* K-12 at high pH and with RpoS induction. Appl Environ Microbiol 84:e00520-18. https://doi.org/10.1128/AEM.00520-18.
46. Kumar S, Tiwari V, Doerrler WT. 2017. Cpx-dependent expression of YqjA requires cations at elevated pH. FEMS Microbiol Lett 364:fnx115. https://doi.org/10.1093/femsle/fnx115.
47. Danese PN, Silhavy TJ. 1998. CpxP, a stress-combative member of the Cpx regulon. J Bacteriol 180:831–839. https://doi.org/10.1128/JB.180.4.831-839.1998.
48. Mitchell AM, Silhavy TJ. 2019. Envelope stress responses: balancing damage repair and toxicity. Nat Rev Microbiol 17:417–428. https://doi.org/10.1038/s41579-019-0199-0.
49. Datsenko KA, Wanner BL. 2000. One-step inactivation of chromosomal genes in *Escherichia coli* K-12 using PCR products. Proc Natl Acad Sci U S A 97:6640–6645. https://doi.org/10.1073/pnas.120163297.
50. Kim YJ, Choi BJ, Park SH, Lee HB, Son JE, Choi U, Chi WJ, Lee CR. 2021. Distinct amino acid availability-dependent regulatory mechanisms of MepS and MepM levels in *Escherichia coli*. Front Microbiol 12:677739. https://doi.org/10.3389/fmicb.2021.677739.
51. Reddy P, Peterkofsky A, McKenney K. 1989. Hyperexpression and purification of *Escherichia coli* adenylate cyclase using a vector designed for expression of lethal gene products. Nucleic Acids Res 17:10473–10488. https://doi.org/10.1093/nar/17.24.10473.
52. Lee HB, Park SH, Lee CR. 2021. The inner membrane protein LapB is required for adaptation to cold stress in an LpxC-independent manner. J Microbiol 59:666–674. https://doi.org/10.1007/s12275-021-1130-8.